

Performance of silicon microdosimetry detectors in boron neutron capture therapy

Peter D. Bradley, Anatoly B. Rosenfeld.

Radiation Physics Group, University of Wollongong, Northfields Ave., Wollongong, NSW, 2522, Australia.

Barry Allen.

St George Hospital, Cancer Care Centre, Gray St, Kogarah, NSW, 2217, Australia

Jeffrey Coderre, Jacek Capala.

Medical Department, Brookhaven National Laboratory, Upton, New York, 11973.

NOTE: Footnotes and Figures are at the end of the file (similar to journal submission form) Figures have been bookmarked use the PDF reader bookmark facility

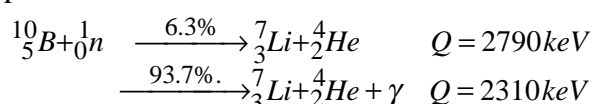
Abstract

Bradley, P.D., Rosenfeld, A.B , Allen, B, Coderre, J., and Capala, J, Performance of silicon microdosimetry detectors in boron neutron capture therapy

Reverse-biased silicon p-n junction arrays using Silicon-On-Insulator technology have been proposed as microdosimeters. The performance of such detectors in boron neutron capture therapy (BNCT) is discussed. This work provides the first reported measurements using boron coated silicon diode arrays as microdosimeters in BNCT. Results are in good agreement with proportional gas counter measurements. Various boron-coating options are investigated along with device orientation effects. Finally, a U-235 coating is tested to simulate device behavior in a heavy ion therapy beam.

I. INTRODUCTION

Boron neutron capture therapy involves the thermal neutron irradiation of a tumor site that has been selectively sensitized to thermal neutrons via the concentration of boron-10 (B-10) within or near cancer cells (*I*). The capture of thermal neutrons by B-10 results in the following nuclear fission process:



The alpha and lithium reaction products are high LET particles that deposit their energy in ranges of 4.1 and 7.7 μm respectively, comparable

to typical mammalian cell dimensions. The energy deposition is highly localized in nature and depends strongly on the subcellular spatial deposition of the B-10 nuclei and the subcellular morphology. In addition to the dose due to B-10 neutron capture, many other dose components are present. Protons are present as recoil products from the interaction of fast and epithermal neutrons with H-1 nuclei and as a product of N-14 neutron capture. Gamma rays arise from H-1 neutron capture and from the neutron source and surrounding materials. Studying complex radiation environments with such localized energy deposition is accomplished using the tools of experimental and theoretical microdosimetry. In particular, experimental microdosimetry provides techniques for separating varying LET components

and measuring dose due to B-10 neutron capture, total dose, beam quality and dose enhancement factors. The separation of LET components using microdosimetric methods is important due to the varying biological effectiveness of these components.

The primary experimental tool for microdosimetric measurements is the proportional gas counter (2). Wu et al. (3) first applied a Rossi type proportional counter to BNCT dosimetry. This has been followed by other studies by Kota¹ and Maughan et al. (4). Although generally considered the best currently available detector, the proportional gas counter has several shortcomings. These include wall effects, a relatively large physical size, phase effects due to measurement in a gaseous phase, and an inability to simulate an array of cells. (2, 5, 6)

McNulty et al. (7) and Roth et al. (8) proposed the use of arrays of silicon reverse-biased p-n junctions for characterizing complex radiation environments inside spacecraft and aircraft. The work was intended to have applications in determining single event upset (SEU) risks to microelectronics and as a biological microdosimeter for personnel monitoring. The detector was used for the separation of neutron irradiation in a mixed radiation field. It is important to note that the detector was based on the deposition of energy by secondary charged particles originating in silicon. Rosenfeld et al. (9) first proposed and demonstrated the use of silicon cells for microdosimetry where the microdosimetric spectra results from secondary charged particles from the irradiated medium.

Silicon array detectors remove several of the previously mentioned problems associated with proportional gas counters. However, the use of silicon diode arrays for microdosimetry has been impeded by two main problems;

1. Tissue equivalency of silicon in microdosimetry and
2. An ill-defined sensitive volume due to diffusion effects and complex charge collection mechanisms.

A previous paper (10) by the authors has addressed the issue of tissue equivalency of silicon based microdosimetric measurements in BNCT.

The analysis was based on a comparative study of range-energy data for H, He, Li and C ions in silicon and tissue. This work demonstrated that under appropriate geometrical scaling (0.63) silicon detectors with well-known geometry will record energy deposition spectra representative of tissue cells of equivalent shape. That is, silicon is tissue equivalent for BNCT under appropriate linear geometrical scaling.

The effects of diffusion may be minimized by appropriate technology selection and device design. Complete characterization of the radiation hardness and sensitive volume of the device used in this study is presented elsewhere (11). However, we note that the use of Silicon On Insulator (SOI) technology in this device significantly improves sensitive volume definition. Based on such promising developments, this work provides the first reported measurements using boron coated silicon diode arrays as microdosimetric detectors in BNCT. The purpose is to present some preliminary results for this new detector technology. The effects of various boron-coating options on microdosimetric spectra are investigated along with device orientation effects. Finally, a U-235 coating is tested to simulate device behavior in a heavy ion therapy beam.

II. MATERIALS AND METHODS

A. Description of Silicon Microdosimeter

The silicon microdosimeter consists of a SOI diode array test structure fabricated by Fujitsu Research Laboratories Ltd.(12). The application requires:

1. An accurately defined sensitive volume (region of charge collection). Minimization of charge collection complexity in particular diffusion and funneling effects.
2. An array of identical diodes to improve collection statistics.
3. Diode structure sizes of the order of a few microns.

An ideal silicon based microdosimeter collects charge in a reverse-biased p-n junction diode via drift driven separation of electron hole pairs in the depletion region. In reality, charge collection is complicated by additional charge collection via

diffusion from outside of the depletion region. By using SOI structures, we preclude any charge collection from beneath the SOI layer due to the underlying insulating layer of SiO₂. Such a design creates a sensitive volume of well-defined depth.

The SOI diode test structures were fabricated on bonded SOI wafers (13) with thicknesses of 2, 5, and 10 μm. The test structures have two different diode arrays with junction sizes of 100×100μm and 10×10μm. In this paper we provide results for the 2 μm SOI device with a junction size of 10×10μm. Table I summarizes array dimensions providing the total N+ junction area and total diode area, including the surrounding P+ junction. Note that all diodes in a given array are connected in parallel.

Table I: Summary of diode array dimensions

Diode Size(um)	Sensitive Volume	Array Size	Total Junction Area	Total Diode Area	Mean Chord Length
10×10	30×30 ×1.7μm	4800 (40×120)	0.48mm ²	4.40 mm ²	3.3μm

The sensitive volume of the device was determined by alpha spectroscopy and ion-microbeam experiments (11). The diode sensitive volume may be approximated by a rectangular parallelepipeds of dimensions 1.7×30×30μm. Note that although the SOI device minimizes diffusion from deep in the substrate the device still collects charge via lateral diffusion. This has two main effects on the dimensions of the sensitive volume:

1. The sensitive volume width and length are increased beyond the junction dimensions
2. Outside of the junction area, charge collection occurs via diffusion and is therefore less efficient than within the junction. Therefore, the charge collection depth, on average, is less than the SOI thickness.

The sensitive volume dimensions are used later in calculating the Mean Chord Length ($MCL=4V/S$, V =volume, S =surface area,(2)) for the microdosimetric spectra.

The N+ and P+ silicon layers with depths 0.2 and 0.5 μm were constructed by arsenic and boron implantation's at 30keV and $5 \times 10^{15} \text{ cm}^{-2}$. The impurity concentration of the P silicon was $1.5 \times 10^{15} \text{ cm}^{-3}$. The device is packaged in a 28 Pin

DIL ceramic carrier. The basic SOI structure is shown in Figure 1. Figure 2 shows the over-layer and detailed device cross-section whilst Figure 3 is a SEM photograph of a portion of the 10×10μm array.

The electronics required for the silicon microdosimeter, as shown in Figure 4, are similar to the proportional gas counter. The device was connected to a Canberra 2003T charge sensitive preamplifier. Noise was minimized by encapsulating the entire microdosimeter probe in an aluminum foil shielding which was then connected to the coaxial cable ground. This also ensured that the chip did not receive any light, which generates significant noise via surface photo-generation. Unlike a proportional counter, the silicon diode array does not require a high voltage supply. The supply voltage used in these experiments varied from 0 to 20V reverse bias.

An 8-meter coaxial cable links the preamplifier to a Canberra 2024 Fast Spectroscopy amplifier. The output of this amplifier is a voltage pulse whose amplitude is proportional to the energy deposited in the sensitive volume of the microdosimeter. Note that the microdosimeter collects charge generated by the traversal of an ion through the device's sensitive volume with the charge collected being proportional to the energy deposited. The pulse height from each event is digitized and stored using a PC based Multi-Channel Analyzer (Ortec, Maestro-model A65-B1, software V3.04).

Calibration of this system was performed using a polonium-210 alpha spectroscopy source with a peak energy of 5.301 MeV. The diode array was replaced by a silicon ion implanted detector that collects charge corresponding to the total energy of the alpha particle. Note that the total gain is insensitive to the detector electrical characteristics since we used a charge sensitive preamplifier. Furthermore, noise performance is not altered by changing detectors because the ion-implanted detector has a similar capacitance to the microdosimeter.

B. Description of Boron and U-235 Coating

Two devices were prepared. One without boron coating and the other with a Lucite coating

containing 1% B-10. The boron coating models the biological situation where boron accumulates on the cell surface (e.g. boron attached to monoclonal antibodies) and we are interested in the microdosimetric spectra within the cell nuclei from a two dimensional array of cells. The device overlayer of between 1-1.35 μm (composed of SiO_2 and Al) crudely represents the cytoplasm spacing between the cell nucleus and surface. The coating was developed by dissolving Lucite shavings in dichloroethane. Decaborane was then added to obtain the required concentration of B-10 to an accuracy of $\pm 5\%$. Drops of the solution were then placed onto the circuit and allowed to dry (~ 20 minutes). Note that extreme care should be taken in this process. Dichloroethane is volatile, its fumes are poisonous, and a mixture of decaborane and dichloroethane is known to be shock sensitive.

The minimum coating thickness required is given by the range (7.4 μm) of a 1.78MeV alpha produced by boron neutron capture. Conversely, too large a thickness may attenuate the thermal neutron fluence. Alpha spectroscopy was performed as an indicator of coating thickness. Since a 5.3MeV alpha has a range in Lucite of 31.9 μm , we would expect no charge collected by the device with a coating greater than this thickness. This was observed after 5 coatings.

However, once coated the device cannot be used for non-boron measurements or alpha spectroscopy experiments. A possible solution is to use a detachable boron coated Lucite lid in close proximity to the detector's surface. A thin Lucite lid with a 1% boron coating was constructed for comparison with the direct coating approach. The air gap between the lid and the detector surface was estimated to be between 100-200 μm .

A third Lucite lid was fabricated with a thin film of aluminum backed Uranium-235 glued to the underside of the lid. U-235 has a high thermal neutron fission cross-section (580 barns). The U-235 nucleus splits in some 40 or so modes following the absorption of a thermal neutron. An average energy of 195 MeV is released in the fission process with a large portion of the energy (162 MeV) carried away by the charged fission fragments. Thus, a U-235 coated lid may be used

to test the microdosimeter's performance under simulated heavy ion treatment conditions.

C. Description of Brookhaven Medical Research Reactor(BMRR)

The 3 MW BMRR is an adjunct to the Medical Research Center of the Medical Department at Brookhaven National Laboratory (BNL). BMRR has three irradiation facilities: an epithermal neutron irradiation facility (ENIF), a thermal neutron irradiation facility, and a broadbeam facility. For this study, we used the ENIF since this beam is used for current clinical trials. A complete description of the facility and collimator design is provided by Liu et al.(14). In our case, a Lucite cubic phantom was positioned at the irradiation treatment port immediately adjacent to the collimator. The center of the cube was aligned to the center of the collimator. The reactor power used for the experiments was 300kW for boron coating measurements and 30kW for the U-238 studies. The thermal neutron flux at 6.5cm depth in a Lucite phantom was calculated (14) as $6.29 \times 10^7 \text{ n/cm}^2/\text{s}$.

D. Description of Phantom

The phantom consists of a sequence of Lucite blocks each 2.5 \times 15 \times 15cm. Using a Lucite nut and bolt, 6 blocks are connected together to form a 15cm sided cube. A similar Lucite cube has been used by us at BNL for previous dosimetry and Monte-Carlo studies. One block is designed with a recess for insertion of the microdosimeter probe. Thus, by rearranging the blocks we may move the probe to different positions within the cube. The primary position for measurements in this paper was 6.5cm depth along the central axis. A 1-meter BNC compatible coaxial cable runs through the probe to connect the microdosimeter to a preamplifier.

E. Microdosimetric measurements

The multi-channel analyzer provides a spectrum of the number of events recorded at different energies. The energy deposited by each event is divided by the mean chord length given in Table I to give the lineal energy (y). To convert to a tissue

equivalent microdosimetric spectrum the mean chord length of the silicon device is simply scaled by a factor of 1/0.63. Thus the diode array is representative of a tissue cell with dimensions $48 \times 48 \times 2.7 \mu\text{m}$ and a mean chord length of $4.8 \mu\text{m}$. Cellular dimensions used in the BNCT literature (15, 16) exhibit a range of values with cellular diameters ranging from $16\text{--}10 \mu\text{m}$ corresponding to mean chord lengths in the range $10.5\text{--}6.5 \mu\text{m}$ (assuming spherical geometry). Thus, the lateral dimensions are larger than typical cell dimensions whilst the mean chord length is slightly less than typical due to the relatively small device thickness.

All microdosimetric spectra are presented in the standard $yd(y) \propto y^2 f(y)$ versus $\text{Log}(y)$ format, where $f(y)$ is the lineal energy probability density distribution calculated from the number of events in the lineal energy range interval dy and $d(y)$ is the dose probability density distribution (5). The ordinate is displayed as $yd(y)$ on a linear-log plot since

$$\int d(y) dy = \ln(10) \int yd(y) d(\log y)$$

and this integral is proportional to the dose deposited in the interval dy . Presented in this way, equal areas under different regions of the function $yd(y)$ correspond to equal doses.

Using the facilities and techniques described in the previous sections microdosimetric spectra were obtained for each coating and lid condition. Experiments were also performed to determine the effect of device orientation on microdosimetric spectra.

III. EXPERIMENTAL RESULTS AND DISCUSSION

A. Evaluation of boron coating methods

A microdosimetric spectrum was obtained for a device with no boron coating in order to determine the influence of boron used in the construction of the device. Boron is used as the p-type dopant in the p+ regions of the chip as discussed in section II.A. The spectrum shown in Figure 5, and scaled by a factor of 100 to compare with a boron coated device, indicates the relatively small contribution from boron fission events within the device's p+ doped region compared to the boron coating. This spectrum also shows the excellent fast neutron filtering of the epithermal beam.

This spectrum also indicates the validity of ion implanting boron directly into the chip in order to simulate boron deposition in various regions of a cell, an idea recently proposed by Rosenfeld et al. (9). Such local B-10 concentration variation is not possible with a proportional gas counter. The p+ region is manufactured by ion implantation of 5×10^{15} boron ions/cm² at an energy of 30 keV and over an area 17% of the total diode area. This gives a B-10 concentration of approximately 1×10^{20} atoms/cm³ or 2000 ppm for 20% isotopic abundance and assuming uniform B-10 distribution within a $0.1 \mu\text{m}$ depth region. Concentrations of 50 ppm, which are equivalent to clinically achievable conditions, could easily be obtained by reducing the implant to 1.2×10^{14} boron ions/cm². The distribution of boron through the cell may also be varied by changing the p+ layout or increasing the substrate boron doping concentration. The latter strategy would require substrate doping of the order of 1.2×10^{19} B-atoms/cm³ to obtain a uniform B-10 concentration of 50 ppm. Note that in the current design thermal neutron interactions with the boron p+ region will greatly exceed reactions with any of the overlayer constituents (Aluminium, Silicon, Oxygen, Titanium and Nitrogen) or the boron within the bulk silicon. This is due to the relatively high thermal neutron capture cross-section of boron and a sufficiently large number of ions implanted.

A comparison was made of the microdosimetric spectra obtained using direct boron coating versus a detachable boron coated lid. As shown in Figure 6, the spectrum for the lid has a comparatively smaller high LET component and a reduced integral count rate. The $100\text{--}200 \mu\text{m}$ air gap when using the lid could account for the reduced high LET component observations. The alpha and lithium ions will typically be past their Bragg peak upon entering the sensitive volume since they must pass through the device overlayer structures. Therefore, any additional overlayer will decrease the total energy deposited.

In summary, direct coating of the chip is the preferred method of boron deposition given the attenuation of energy in the air gap and the possible large variation in the air gap distance

using the lid method. Based on these observations, the coated device was used for the remainder of this work.

The acquisition time for the spectra obtained in Figure 6 and Figure 5 was only 3 minutes at 300 kW reactor power. The ability of the silicon microdosimeter to function at full reactor power is an additional advantage over the proportional gas counter.

B. Evaluation of device orientation effects

In order to determine the sensitivity of the device to beam orientation, the Lucite phantom was rotated with the detector positioned in the center of the phantom. The horizontal detector position gave a reduction in integral counts of 6.8% when compared to the vertical with minimal changes in spectral character. Thus, the device is relatively insensitive to orientation. This result is to be expected given the isotropic nature of thermal neutrons.

C. Measurement using U-235 coated diode array

Measurements were performed on the diode array with a small piece of U-235 coated aluminum foil placed on the underside of a Lucite lid. The lid fits onto the recess in the device package, which contains the diode array. The air gap distance between the foil and device is estimated at between 200-300 μ m. The fragments produced by the U-235 fission are heavy ions which produce dense plasma tracks in the silicon. Thus, the device must be sufficiently reverse biased to minimize recombination of electron-hole pairs in the plasma track. The purpose of this experiment was to determine the required reverse bias for heavy ions. This provides valuable information for future experiments at heavy ion therapy facilities. Figure 7 indicates that for voltages greater than 5 volts the difference between spectra is minimal. Therefore, under heavy-ion conditions, the minimum recommended bias voltage is approximately 5 volts, although higher voltages give slightly improved performance. Note that at zero bias recombination significantly reduces the charge collected by the microdosimeter.

IV. COMPARISON WITH SIMULATION

Bradley and Rosenfeld (10) have reported the development of a Monte-Carlo program to model BNCT energy deposition in various rectangular parallelepiped (RPP) geometries. The materials modeled include tissue and silicon. The program randomly selects thermal neutron interaction points and ion emission angles within a RPP geometry called the generation volume. The energy deposited in another RPP geometry called the sensitive volume is calculated by integrating LET along the chord length traversed by the lithium and alpha ions.

This program is suitable for some preliminary simulations of the expected microdosimetric spectra. The simulations indicate a reasonable agreement with experimental results as shown in Figure 8. However, the Monte-Carlo program is simplistic in many respects including (in order of expected importance (11)):

1. The program does not appropriately model lateral charge diffusion and assumes complete charge collection in an idealistic RPP geometry.
2. Variations in overlayer structures are neglected. The overlayer is assumed uniform in thickness and composition.
3. Ion range straggling and energy straggling is neglected.
4. Electrical noise components are assumed to be zero.

Inclusion of all of these effects will broaden the spectra, which should improve the correspondence between theory and experiment. Of particular importance is the variation attributed to non-uniform collection efficiency, which may reduce to almost 55% for points distant from the central n+ junction (11). These issues will be addressed in a future version of the Monte-Carlo software.

V. COMPARISON WITH PROPORTIONAL COUNTER MICRODOSIMETRIC MEASUREMENTS

Only two studies have been performed using proportional gas counters to measure BNCT microdosimetric spectra. The study performed by Wu et al. (3) is most appropriate for comparison with the diode array since both measurements

were performed at BMRR. Wu performed measurements using a 2.5cm spherical TE proportional gas counter with 50ppm TE walls and gas. Site diameters of 2 and 6 μ m, corresponding to mean chord lengths of 1.3 and 4 μ m, were simulated by varying gas pressure.

Figure 9 provides a comparison of these measurements with the diode array. The spectra show similar peaks although a direct comparison with the diode array is difficult since the mean chord length of the diode array is about 3 μ m and the pattern of boron deposition differs significantly between detectors. Boron deposition is throughout the entire detector for the proportional counter whilst only on the surface of the diode array. Differences in the spectra may be expected primarily due to different chord-length distributions between a spherical counter geometry and the diode array's RPP type geometry. Wu's device contains boron within the counter so "starters" and "insiders" are included whilst the boron coated diode array measures only "crossers" and "stoppers" (See (17) for terminology). Furthermore, the diode array overlayer of 1.2 μ m (on average) separates the boron from the detector. This will reduce somewhat the energy of alpha and lithium ions as well as altering the chord length distribution. Such effects account for the lower lineal energy recorded by the diode array.

VI. SUMMARY AND CONCLUSIONS

This paper demonstrates the first application of silicon p-n junction SOI arrays for microdosimetry in radiation oncology and particularly for BNCT. The SOI technology provides a well-defined sensitive depth, although design improvements are required to minimize lateral diffusion effects. Coating of the device with various converters (Lucite with B-10 and U²³⁵) was investigated. Direct coating of the device with 1%B-10 in Lucite did not change electrical characteristics and provided a microdosimetric spectra consistent with simulations. In addition, preliminary results with the U²³⁵ converter suggest that the SOI p-n junction is a promising microdosimeter for heavy ion therapy. This will be experimentally verified in a heavy ion clinical facility. Measurement of the spectra generated from B-10 deposited within the

device p+ regions demonstrated that typical medical concentrations of B-10 may be introduced in the device design via ion implantation. Such a microdosimeter may be used under full reactor power with any device orientation.

The silicon diode array is intended as an alternative to the proportional gas counter for experimental microdosimetry. The diode array is a low cost system without the need for gas flow technology and high voltage supplies. The diode array offers such advantages as a measurement in the solid phase and thus removal of wall effects, simulation of a two dimensional array of cells for improvement in collection statistics, small physical size, high spatial resolution and operation at clinical reactor power settings. Furthermore, the possibility exists that future devices may be constructed with sizes and morphology more nearly representative of biological cells, specific boron implantation in various cell/diode regions and simultaneous macrodosimetry on the same device. The construction of such devices may exploit the rapid development and current manufacturing capabilities of silicon based integrated circuit technology.

In response to the failure of traditional microdosimetry to adequately represent realistic tissue architecture and boron distribution, Solares and Zamenhof (18) have developed high-resolution quantitative autoradiography. This technique is difficult and time consuming, although it is currently the most realistic microdosimetric technique available. However, the improvements in traditional microdosimetry possible using silicon diode arrays may help to bridge the gap between proportional counter microdosimetry and the more realistic autoradiography method.

ACKNOWLEDGMENTS

The authors would like to thank Shigeo Satoh of Fujitsu Research Laboratories for providing the diode array samples and the staff of BNL medical research reactor for their generous time and effort. We are also indebted to John Burke (University of Wollongong) for his outstanding skills in manufacturing the Lucite probes, P Litovehenko (KINR) for the U²³⁵ converter and James Ziegler

(IBM) for the latest copy of SRIM. This work was funded by Australian National Health and Medical Research Council Grant No 960804 and an Australian Department of Industry, Science and Technology grant.

FOOTNOTES

1. C. Kota, PHD dissertation: *Microdosimetric considerations in the use of the boron neutron capture reaction in radiation therapy*, Wayne State University, Detroit, 1996.

REFERENCES

1. B. Larsson, J. Crawford and R. Weinrich, Eds., *Advances in Neutron Capture Therapy, Volume I: Medicine and Physics*. Elsevier, Zürich, 1996.
2. International Commission on Radiation Units and Measurements, *Microdosimetry (ICRU report; 36)* ICRU, Maryland, 1993.
3. C. S. Wu, H. I. Amols, P. Kliauga, L. E. Reinstein and S. Saraf, Microdosimetry for Boron Neutron Capture Therapy. *Radiat. Res.* **130**, 355-359 (1992).
4. R. L. Maughan, M. Yudelev and C. Kota, A microdosimetric study of dose enhancement in a fast neutron beam due to boron neutron capture therapy. *Phys. Med. Biol.* **38**, 1957-1961 (1993).
5. H. H. Rossi and M. Zaider, *Microdosimetry and Its Applications* Springer, London, 1996.
6. A. M. Kellerer, Event simultaneity in cavities. Theory of the distortions of energy deposition in proportional counters. *Radiat. Res.* **48**, 216 (1971).
7. P. J. McNulty, D. R. Roth, E. G. Stassinopoulos and W. J. Stapor, Characterizing complex radiation environments using MORE (monitor of radiation effects), T. Dombek, V. Kelly and G. P. Yost, Eds., Symposium Detector Research and Development., SSC World Scientific, 1990.
8. D. R. Roth, P. J. McNulty, W. J. Beauvais, R. A. Read and E. G. Stassinopoulos, Solid-state microdosimeter for radiation monitoring in spacecraft and avionics. *IEEE Trans. Nucl. Sci.* **41**, 2118-2124 (1994).
9. A. B. Rosenfeld, G. I. Kaplan, M. G. Carolan, B. J. Allen, R. Maughan, M. Yudelev, C. Kota and J. Coderre, Simultaneous macro-micro dosimetry with MOSFETs. *IEEE Trans. Nucl. Sci.* **43**, 2693-2700 (1996).
10. P. D. Bradley and A. B. Rosenfeld, Tissue Equivalence Correction for Silicon Microdosimetry Detectors in Boron Neutron Capture Therapy. *Med. Phys.* (In press-1998).
11. P. D. Bradley, A. B. Rosenfeld, K. K. Lee, D. Jamieson and S. Satoh, Charge collection and radiation hardness of a SOI microdosimeter for space and medical applications. *IEEE Trans. Nucl. Sci.* **45** (In press 1998).
12. Y. Tosaka, S. Satoh, K. Suzuki, T. Sugii, N. Nakayama, H. Ehara, G. A. Woffinden and S. A. Wender, Measurements and Analysis of Neutron-Reaction-Induced Charges in a Silicon Surface Region. *IEEE Trans. Nucl. Sci.* **44**, 173-178 (1997).
13. J. B. Lasky, Wafer bonding for silicon-on-insulator technologies. *Appl. Phys. Lett.* **48**, 78 (1986).
14. H. B. Liu, D. D. Greenberg, J. Capala and F. J. Wheeler, Improved neutron collimator for brain tumor irradiations in clinical boron neutron capture therapy. *Med. Phys.* **23**, 2051-2060 (1996).
15. T. Hartman and J. Carlsson, Radiation dose heterogeneity in receptor and antigen mediated boron neutron capture therapy. *Radiotherapy and Oncology.* **31**, 61-75 (1994).
16. T. Nguyen, G. L. Brownell, S. A. Holden, S. Kahl, M. Miura and B. A. Teicher, Subcellular distribution of various boron compounds and implications for their efficacy in boron neutron capture therapy by Monte Carlo simulations. *Radiat. Res.* **133**, 33-40 (1993).
17. R. S. Caswell, Deposition of energy by neutrons in spherical cavities. *Radiat. Res.* **27**, 92-107 (1966).
18. G. R. Solares and R. G. Zamenhof, A novel approach to the microdosimetry of neutron capture therapy. Part I. High-resolution quantitative autoradiography applied to microdosimetry in neutron capture therapy. *Radiat. Res.* **144**, 50-58 (1995).

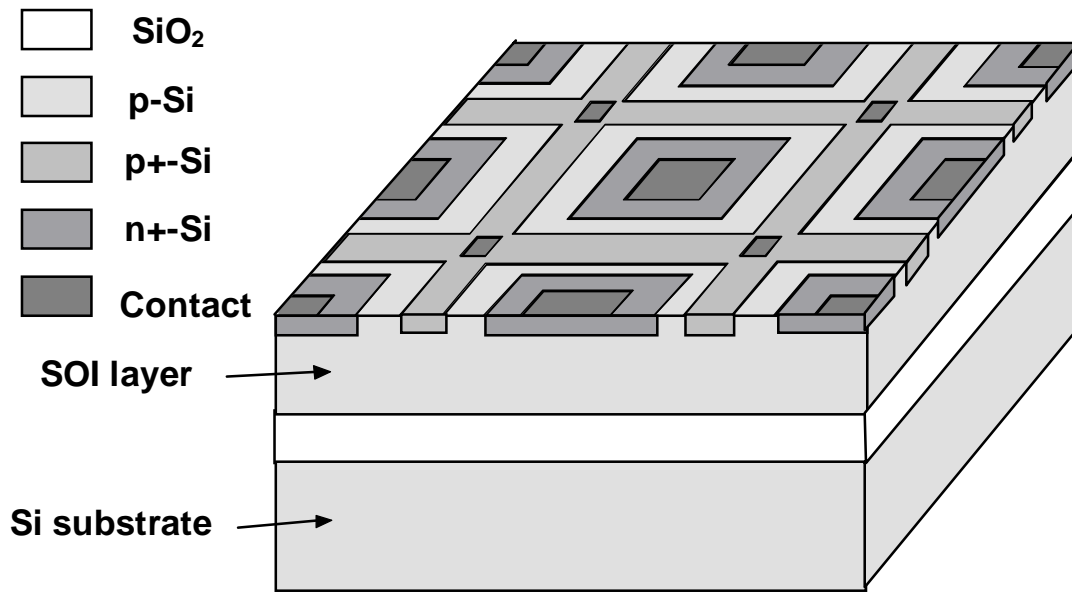


Figure 1: Basic SOI diode array structure. Layout shown is approximate only.

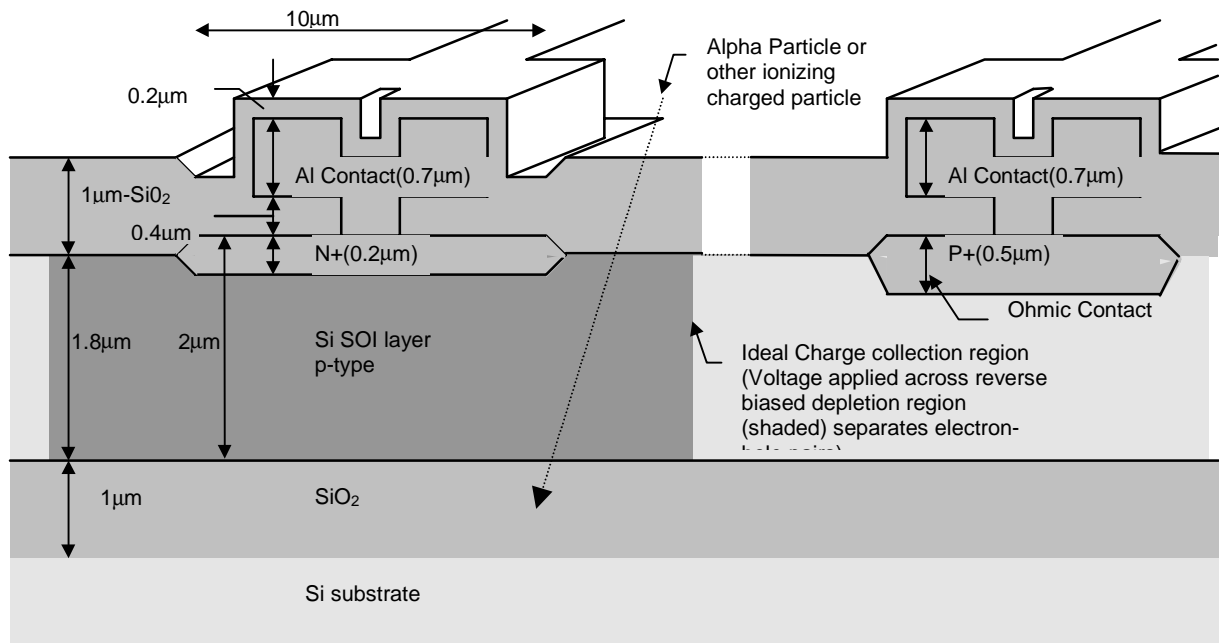


Figure 2: Detailed cross-section of diode array with approximate dimensions. For simplicity, the p+ and n+ contacts are shown aligned although Figure 3 provides a more accurate representation of their relative alignment.

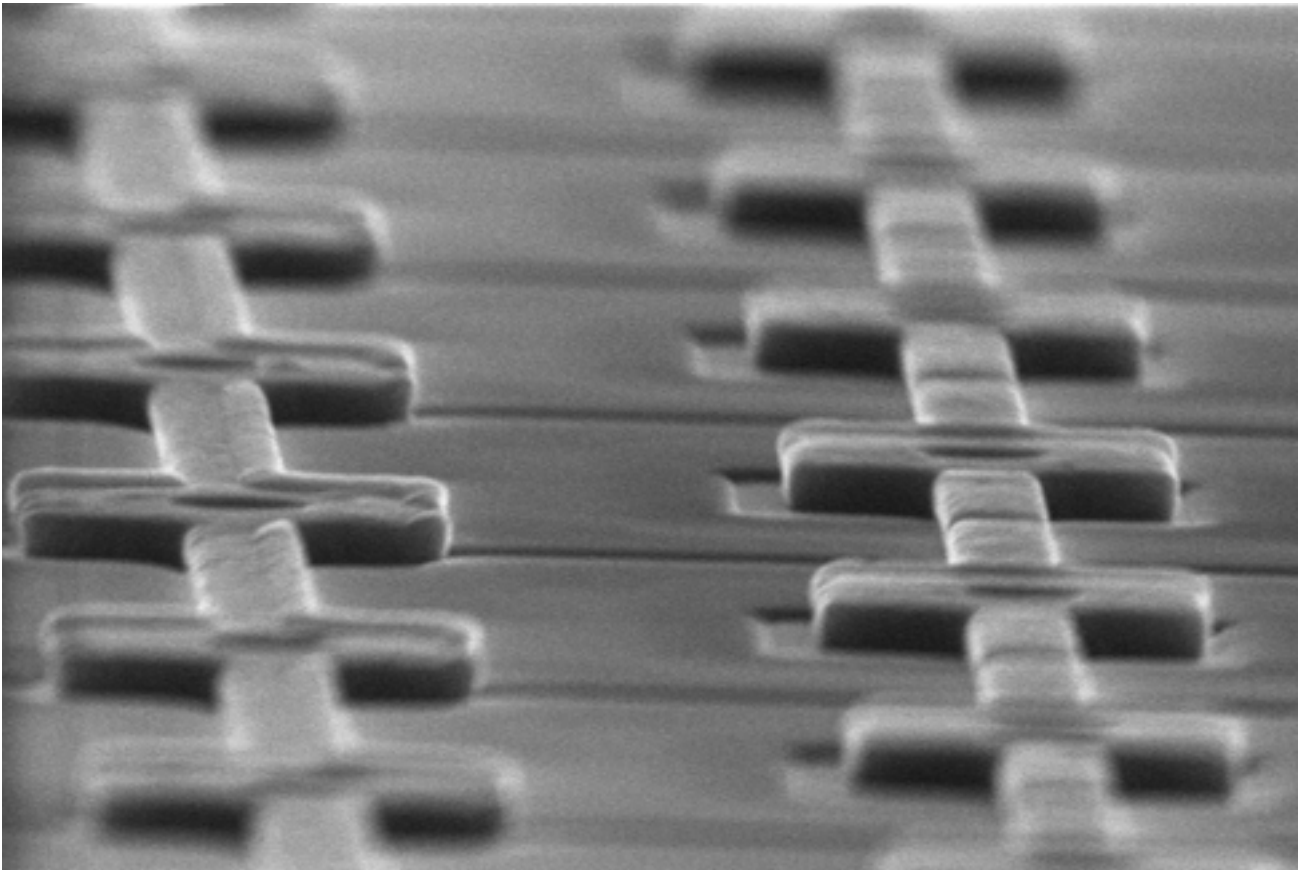


Figure 3: SEM photograph of a portion of the $10 \times 10 \mu\text{m}$ diode array. (Note: Raised sections are aluminum tracks connecting contacts so that all diodes are electrically in parallel. The n^+ contacts are on the right whilst the p^+ contacts are shown on the left side. The width of the photo is about $23 \mu\text{m}$.)

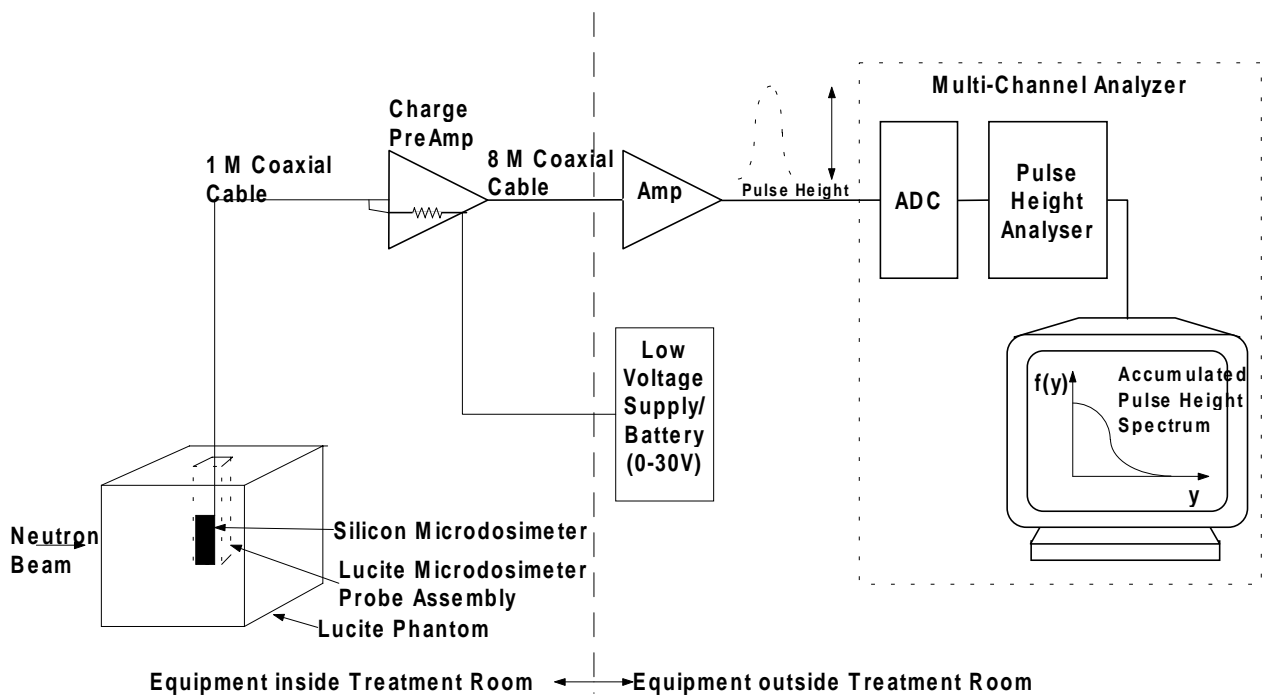


Figure 4: Experimental setup for microdosimetry measurements

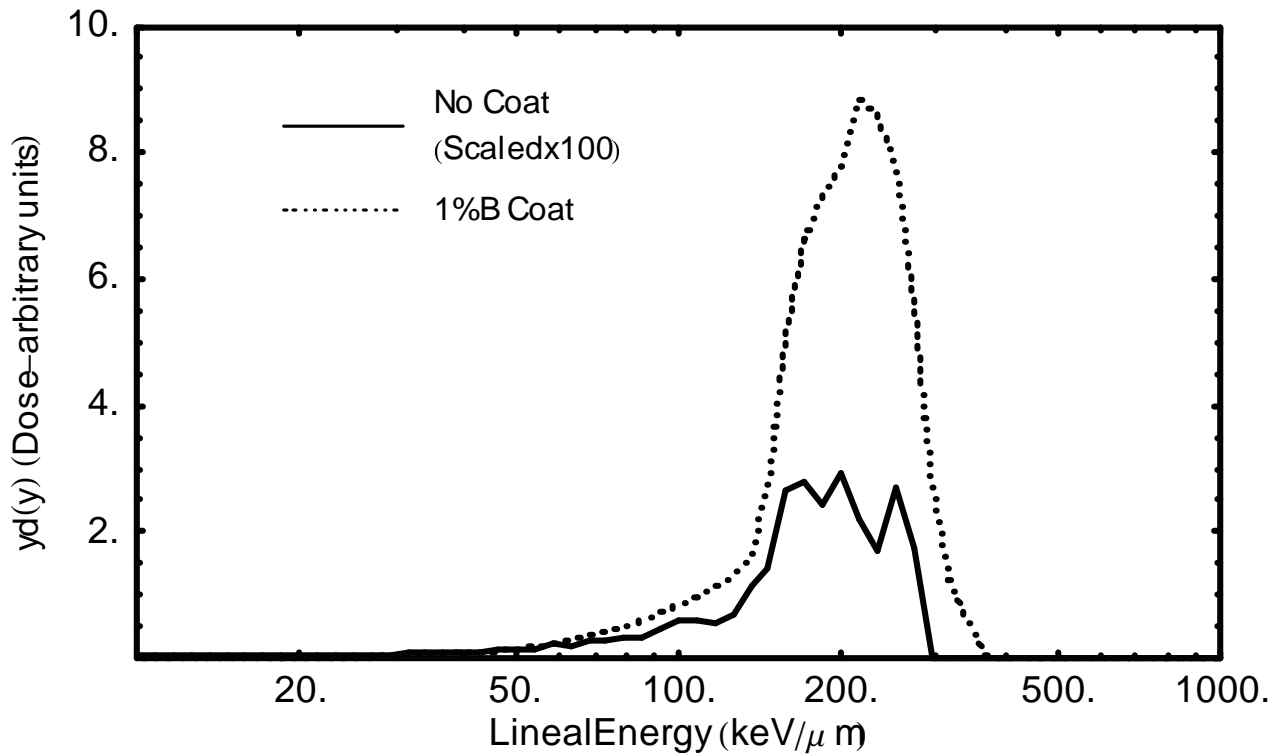


Figure 5: Microdosimetric spectra for non-boron coated device compared with boron coating. The spectra were obtained at a depth of 6.5cm in the Lucite phantom with a reactor power of 300kW. Note that the no coat spectrum is scaled up by a factor of 100. The peak at 200 keV/ μ m in the no coat spectrum arises from boron p+-dopant in the device.

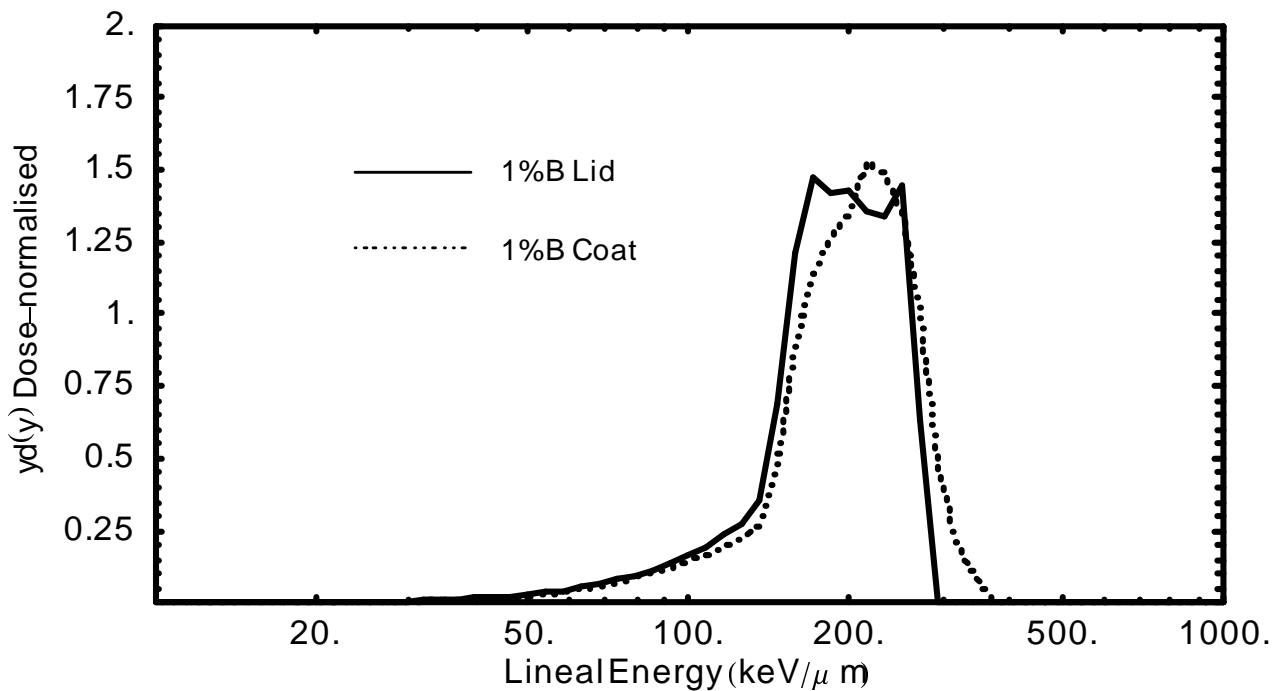


Figure 6. Microdosimetric spectra for various coating options. The spectra were obtained at a depth of 6.5cm in the Lucite phantom with a reactor power of 300kW.

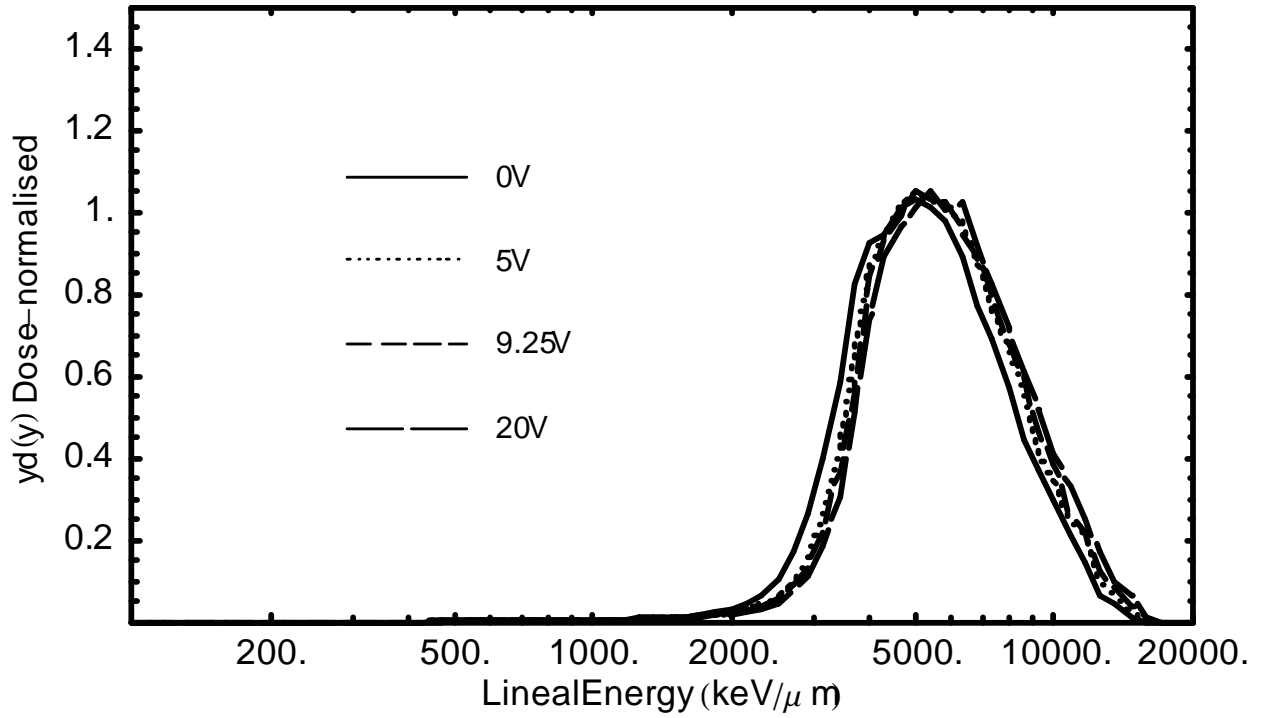


Figure 7. Bias dependence of U-235 Covered diode array at a depth of 6.5cm in Lucite phantom, Reactor Power=30kW

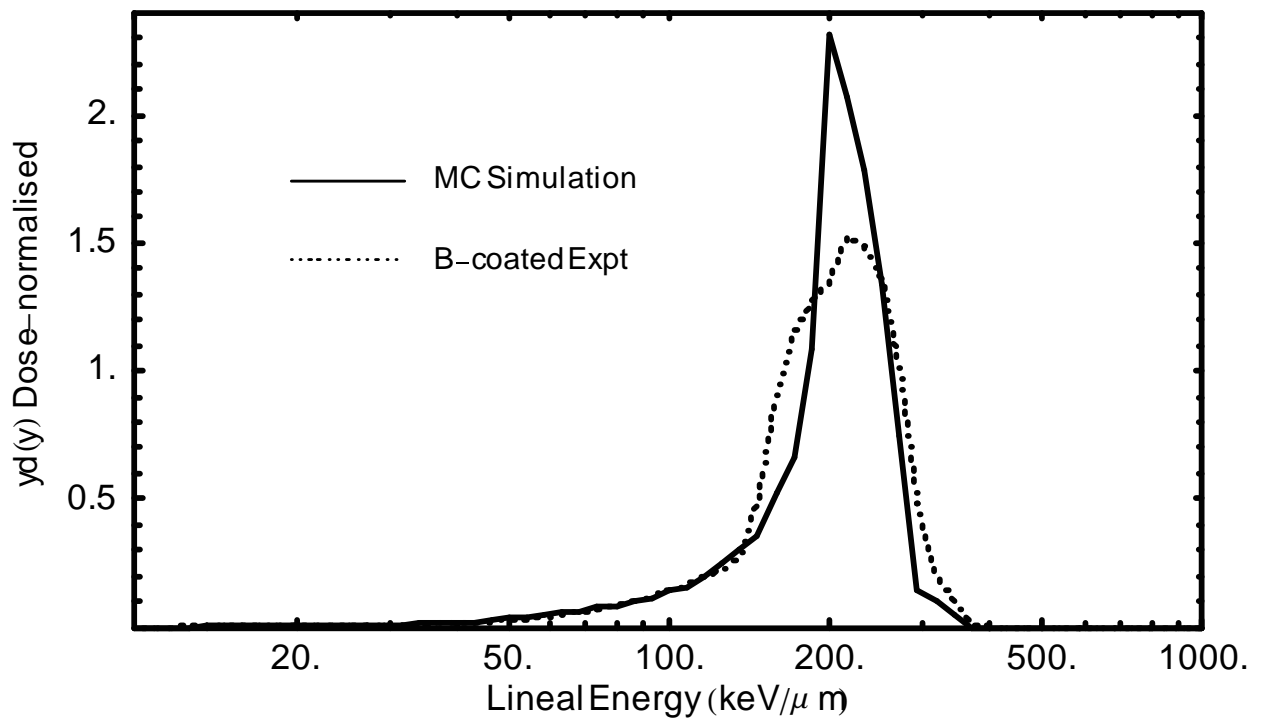


Figure 8: Comparison of experimental results (1% B coated diode array (10x10μm) at 6.5cm) with Monte-Carlo Simulation

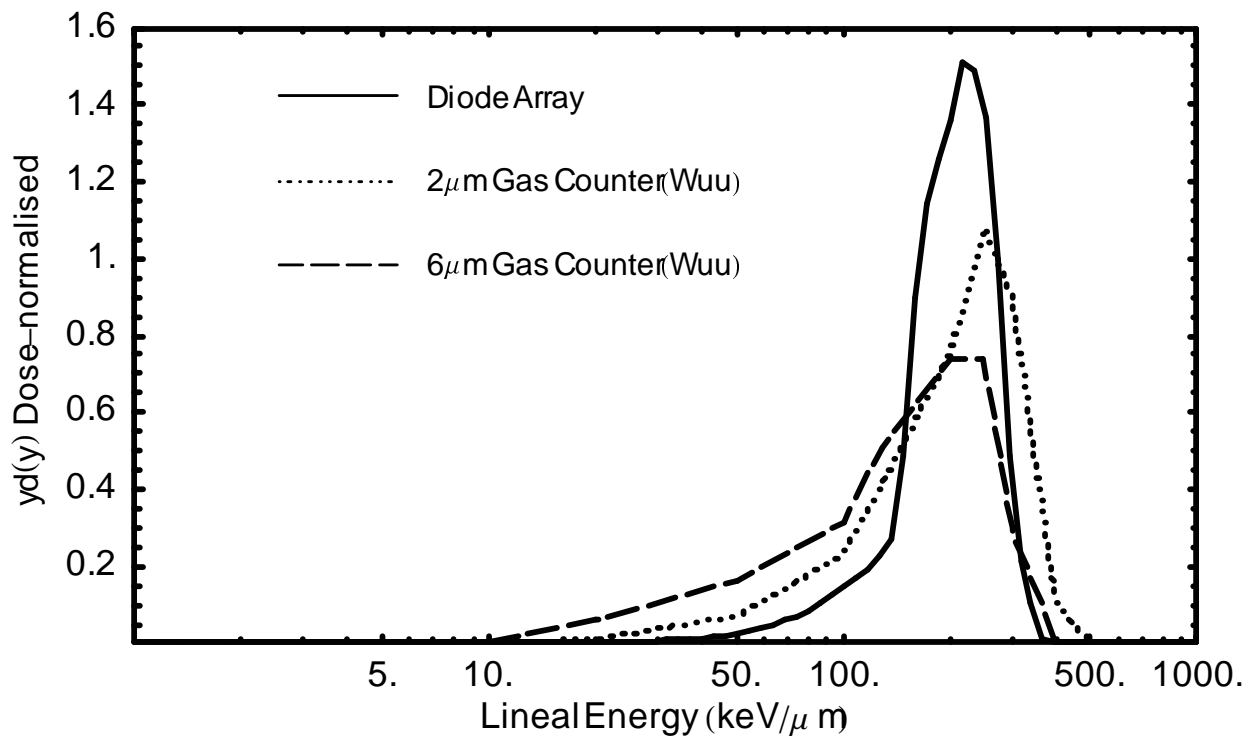


Figure 9: Comparison of proportional counter (3) with diode array at BMRR.